Proceedings Paper:
Liu, J, Richardson, R, Hewson, R et al. (1 more author) (2015) Mechanical Design of Long Reach Super Thin Discrete Manipulator for Inspections in Fragile Historical Environments. In: Dixon, C and Tuyls, K, (eds.) Lecture Notes in Computer Science. Towards Autonomous Robotic Systems 16th Annual Conference, TAROS 2015, 08-10 Sep 2015, Liverpool, UK. Springer Verlag , pp. 155-160. ISBN 978-3-319-22415-2

https://doi.org/10.1007/978-3-319-22416-9_18

Mechanical Design of Long Reach Super Thin Discrete Manipulator for Inspections in Fragile Historical Environments

Jason Liu[1], Robert Richardson[1], Rob Hewson[2] and Shaun Whitehead[3]

[1] School of Mechanical Engineering, University of Leeds, Leeds, United Kingdom
{mn07jhwl, r.c.richardson}@leeds.ac.uk
[2] Faculty of Engineering, Imperial College, London, United Kingdom
r.hewson@imperial.ac.uk
[3] Scoutek Ltd., Saltburn-by-the-Sea. United Kingdom
shaun@scoutek.com

Abstract. Long reach and small diameter manipulators are ideal for borehole deployments into search and rescue scenarios and fragile historical environments. Small diameter passageways impose constraints on a snake arm manipulator which severely limit its performance and capabilities. This work investigates the effects of tendon tensions on the maximum working length of a snake arm under tight size constraints and how the maximum length is achieved through an algorithmic approach and consideration of how and when key parts fail.

Keywords: Exploration, Long reach, Discrete backbone, Robot archaeology, Snake arm, Tendon tension, Minimally invasive, Small Diameter

1 Introduction

The application of robotic devices has been widely used in exploration and search and rescue (SAR) scenarios [1]. Ideally deployed where human risk is considered too high [2], tools such as the snake arm are often important for examining confined space environments where humans and some robots struggle. These robotic platforms are profoundly influenced by their intended environments and most exploit a single locomotion mechanism to operate in the complex terrains [3-5].

Different environments greatly vary from one to another, and produces a level of uncertainty and challenges for the end user [4]. It can be desirable for small boreholes to be used as means of access. Small boreholes will be faster to drill and reduces secondary collapse hazards; they are also less destructive and aid to preserve a site. Snake arms already have all the necessary locomotion parts anchored to a mobile platform outside the borehole [6-8], this allows the snake arm to fully utilize a boreholes diameter which plays a vital role in the snake arm's length.

The length of a snake arm is representative of the maximum working distance possible with a manipulator. Current small diameter snake arms include the continuous DTRA arm by OC Robotics with a reach of 610 mm and an outer diameter of 12.5 mm [9]. On the other hand long reach snake arms with large diameters already exist where mechanisms to compensate for gravity are possible to achieve unsupported lengths of 6 m with a 100 mm diameter [9].

In this paper the design of a triple jointed snake arm manipulator that conforms to a very restrictive small diameter constraint is firstly introduced, and then an analysis of the snake arm theory is discussed. Lastly, an algorithmic approach is used to determine the maximum working length for the snake arm.

2 Description of the Basic Snake Arm

A discrete backbone snake arm simplifies kinematic formulations and motion control over its continuous backbone counterpart [16]. Formed from a series of links and joints and actuated by a minimum of three tendons per joint, those tendons run through each link and terminate at each joint it is assigned to control. Assuming the boreholes are straight, the snake arm is not expected to maneuver around obstacles until it breaches through the borehole into a target chamber.

A snake arm capable of self-supporting the full length of its own arm in the deployed environment is advantageous for surveying fragile and historically important tomb-like chambers because there would be no need for any contact between the arm and surfaces for any risk of damage to occur. Fig. 1 shows a 12 mm diameter snake arm consisting of a base link (of length B), three two degrees of freedom (DOF) joints (of length J) and three links of identical length (of length L). The diameter places physical constraints on the number of cables controlling the snake arm joints, the thickness of the tubing that makes the links and the diameter of the two DOF joints.

Increasing link length L to create a longer snake arm has the effect of increasing the tendon tensions required to maintain the snake arms horizontal cantilever position. These forces result in greater axial compressive forces acting through the snake arm and possibly leading to joint failure and/or buckling of the links.

As a consequence, a method was required to theoretically calculate the tendon tensions from the snake arms kinematics and analyze the values to determine whether any anticipated failure modes will occur.

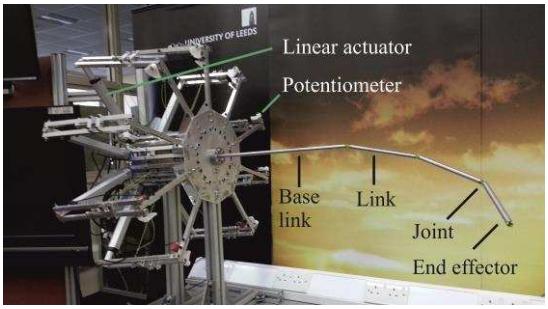

Fig. 1. 12 mm diameter snake arm

3 Discrete Snake Arm Kinematics and Statics

The position of the end effector with respect to the base frame is computed with forward kinematics using transformation matrices produced from joint angles and link lengths. Combined with the Recursive Newton-Euler (RNE) method the toque at each joint is computed and carried over to calculate the cable tensions.

The RNE joint torques reaches a maximum when the snake arm is at a horizontal cantilever position without additional external forces other than gravity acting upon it; therefore at this point it is assumed the associated tendon tensions are also at its maximum. This horizontal state should then be where failure of the snake arm is most likely to occur and is where this analysis is focused on.

Calculating tendon tensions from joint torques can be performed if tensions are assumed constant throughout with negligible friction and all joint angles are known. For a snake arm with two joints and two tendons of link length L, weight W, payload weight P and perpendicular tendon distance of Dy as shown in Fig. 3, multiple tendons cannot occupy the same space for all joints, therefore some tendons are displaced radially about the center. This creates an undesirable lateral load and requires the introduction of additional tendons to counteract the loads.

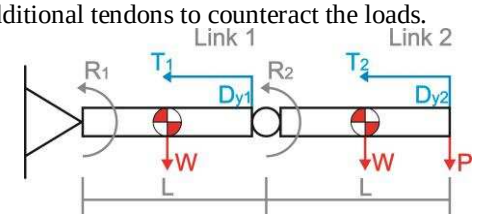

Fig. 3. Simplified snake arm with two joints and two tendons

The RNE method is used to calculate the joint torques R_1 and R_2 and the tendon tensions calculated for the ith joint is expressed as:

$$R_{xy}i = \sum_{j=i}^{N} T_j \, D_{xy}j \tag{1}$$

Where $R_{xy}i$ is the torque generated at joint i for both yaw (R_x) and pitch (R_y) joint directions. T_j is the tension of each tendon that passes through or terminates at joint j. $D_{xy}j$ is defined as the distance between tendon j and the neutral axis of joint i, it can also be a negative value dependent on the direction the tendon j transmits its force on joint i. Applying equation (1) to the double jointed snake arm as shown on Fig. 3, the equations relating torques to tensions can be produced and solved using matrices.

$$\begin{bmatrix} 0 & D_{y2} \\ D_{y1} & D_{y2} \end{bmatrix} \begin{bmatrix} T_1 \\ T_2 \end{bmatrix} = \begin{bmatrix} R_{y2} \\ R_{y1} \end{bmatrix} \tag{2}$$

Where the tensions T_1 and T_2 can be solved as:

$$\begin{bmatrix} T_1 \\ T_2 \end{bmatrix} = \begin{bmatrix} \frac{R_{y1}}{D_{y1}} - \frac{R_{y2}}{D_{y1}} \\ \frac{R_{p2}}{D_{y2}} \end{bmatrix} \tag{3}$$

For a three jointed snake arm with six DOF and nine control tendons, equation (1) creates a system of linear equations with infinite solutions.

$$\begin{bmatrix} 0 & 0 & D_{x3} & 0 & 0 & D_{x6} & 0 & 0 & D_{x9} \\ 0 & 0 & D_{y3} & 0 & 0 & D_{y6} & 0 & 0 & D_{y9} \\ 0 & D_{x2} & D_{x3} & 0 & D_{x5} & D_{x6} & 0 & D_{x8} & D_{x9} \\ 0 & D_{y2} & D_{y3} & 0 & D_{y5} & D_{y6} & 0 & D_{y8} & D_{y9} \\ D_{x1} & D_{x2} & D_{x3} & D_{x4} & D_{x5} & D_{x6} & D_{x7} & D_{x8} & D_{x9} \\ D_{y1} & D_{y2} & D_{y3} & D_{y4} & D_{y5} & D_{y6} & D_{y7} & D_{y8} & D_{y9} \end{bmatrix} \begin{bmatrix} T_1 \\ T_2 \\ T_3 \\ T_4 \\ T_5 \\ T_6 \\ T_7 \\ T_8 \\ T_9 \end{bmatrix} = \begin{bmatrix} R_{y3} \\ R_{x3} \\ R_{y2} \\ R_{x2} \\ R_{y1} \\ R_{x1} \end{bmatrix} \tag{4}$$

As the tendons with a negative D_y would not contribute to overcoming the gravity acting on the snake arm, these can be given pre-tension values and this action results in a solvable matrix and the necessary equations for a theoretical tendon tensions.

$$\begin{bmatrix} 0 & 0 & D_{x3} & 0 & 0 & D_{x9} \\ 0 & 0 & D_{y3} & 0 & 0 & D_{y9} \\ 0 & D_{x2} & D_{x3} & 0 & D_{x8} & D_{x9} \\ 0 & D_{y2} & D_{y3} & 0 & D_{y8} & D_{y9} \\ D_{x1} & D_{x2} & D_{x3} & D_{x4} & D_{x8} & D_{x9} \\ D_{y1} & D_{y2} & D_{y3} & D_{y4} & D_{y8} & D_{y9} \end{bmatrix} \begin{bmatrix} T_1 \\ T_2 \\ T_3 \\ T_4 \\ T_8 \\ T_9 \end{bmatrix} = \begin{bmatrix} R_{y3} - T_6 D_{x6} \\ R_{x3} - T_6 D_{y6} \\ R_{y2} - T_5 D_{x5} - T_6 D_{x6} \\ R_{x2} - T_5 D_{y5} - T_6 D_{y6} \\ R_{y1} - T_5 D_{x5} - T_6 D_{x6} - T_7 D_{x7} \\ R_{x1} - T_5 D_{y5} - T_6 D_{y6} - T_7 D_{y7} \end{bmatrix} \tag{5}$$

The tensions T_5, T_6 and T_7 in (5) are the pre-tension values assigned, where a value of zero would represent the tendon left slack.

4 Cable Tension Experiment

To measure the tension of the tendons in multiple configurations, a test rig modelled after Fig. 3 was assembled with two single DOF joints and links of constant length with capacity for five joints and fifteen tendons at three different diameters.

The methods consisted of holding the arm at a horizontal cantilever position and incrementally attach weights to each tendon. When the arm is released and maintains its position with no change to joint angles the weight is recorded and the process repeated. If inadequate tension is supplied to the tendons the arms would collapse and if too much tension is supplied the arm will rise beyond the horizontal starting position. To alter the torque at each joint only the payload was incremented.

The results shown on Fig. 4 show a close trend between the theoretical equation (3) and the experimental results. Further investigation revealed the zero-shift in the data was the result of friction in the test rig between the tendon, vertebra and pulleys and the theoretical calculations which were assumed to have negligible. To compensate for the error, the relationship between the load acting on the tendons and friction for the test rig was measured with the experimental values adjusted for the additional friction forces dependent on the load on the tendons.

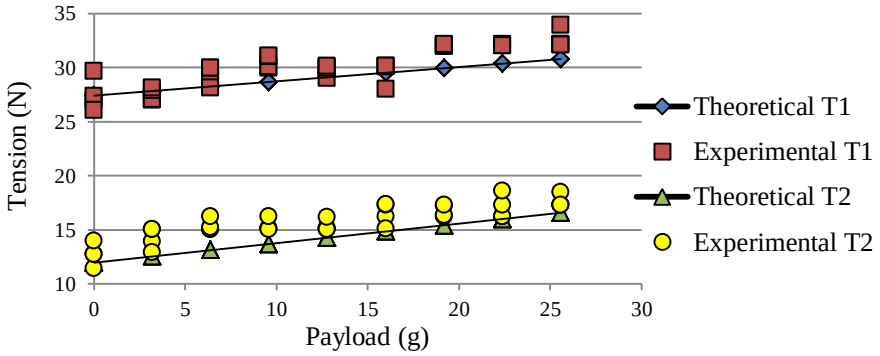

Fig. 4. Comparison between theoretical and experimental tendon tensions for a double jointed snake arm with two tendons.

5 Maximum working length

MATLAB was used to determine the maximum length of snake arm by algorithmically increasing the length of both links whilst at each step checking against the anticipated failure modes (Table 1). The implementation of factors of safety (FOS) reduces the lengths as a compromise for increased reliability.

The approach was to firstly determine the maximum length of the Links and thereafter determine the length of the Base link. This is because the Base link length does not affect the tendon tensions, the calculations for buckling failure of the three Links or the forces acting onto the 2DOF joints. However the axial stress resulting from the tendon tensions acting through the Base link and weight of the unsupported snake arm does affect the likelihood of buckling for the Base link.

Strongly dependent on the design of the snake arm, the order the failure modes will materialize is difficult to determine and so each mode was analysed individually in the design.

Table 1. Anticipated snake arm failure modes and Factors of Safety

Failure Mode	Check	FOS
Tendon	Each calculated tendon tension was compared to the tendons experimentally found yield stress.	6
Joints	Using Finite element analysis to find the load required for joint failure and compare to the predicted compressive axial loads.	4
Link Buckling	Axial stress through the links was analyzed for buckling using buckling theory for thin walled cylinders in axial compression [10,11].	4

This approach yielded a snake arm of total length 1.011m with a Link length of 0.161m and Base link of 0.478m for the 12mm diameter snake arm.

6 Conclusion and Future Work

The limiting factors for the design of the snake arm were the tendons and link buckling. A length of 1.676 m is achieved if the FOS is set to the point of failure. However a better approach would be to increase the yield stress of the tendons and design links capable of greater compressive loads. The outcome of the algorithmic approach to find the maximum length resulted in a length of 1.011m making this design not ideal for SAR scenarios where much greater lengths are crucial but possible for archeology.

In future, the snake arm will be examined to increase reach. Including an investigation into the effect of axial, bending, and twisting forces through the joints and lastly, further tests by performing fielded experiments in real world situations.

References

1. Jueyao, W., Xiaorui, Z., Fude, T., Tao, Z., Xu, X.: Design of a modular robotic system for archaeological exploration. In: Robotics and Automation, 2009. ICRA '09. IEEE International Conference on, 12-17 May 2009 2009, pp. 1435-1440
2. Guizzo, E.: Robots Enter Fukushima Reactors, Detect High Radiation http://spectrum.ieee.org/automaton/robotics/industrial-robots/robots-enter-fukushima-reactors-detect-high-radiation (2011)
3. Daler, L., Lecoeur, J., Hahlen, P.B., Floreano, D.: A flying robot with adaptive morphology for multi-modal locomotion. In: Intelligent Robots and Systems (IROS), 2013 IEEE/RSJ International Conference on, 3-7 Nov. 2013 2013, pp. 1361-1366
4. Morris, A., Ferguson, D., Omohundro, Z., Bradley, D., Silver, D., Baker, C., Thayer, S., Whittaker, C., Whittaker, W.: Recent developments in subterranean robotics. Journal of Field Robotics **23**(1), 35-57 (2006)
5. Murphy, R.R., Kravitz, J., Stover, S., Shoureshi, R.: Mobile robots in mine rescue and recovery. Robotics & Automation Magazine, IEEE **16**(2), 91-103 (2009)
6. Hirose, S.: Biologically inspired robots : snake-like locomotors and manipulators. Oxford University Press, (1993)
7. Buckingham, R.O., Graham, A.C.: Dexterous manipulators for nuclear inspection and maintenance - Case study. In: Applied Robotics for the Power Industry (CARPI), 2010 1st International Conference on, 5-7 Oct. 2010 2010, pp. 1-6
8. Junhu, H., Rong, L., Ke, W., Hua, S.: The mechanical design of snake-arm robot. In: Industrial Informatics (INDIN), 2012 10th IEEE International Conference on, 25-27 July 2012 2012, pp. 758-761
9. Chalfoun, J., Bidard, C., Keller, D., Perrot, Y., Piolain, G.: Design and flexible modeling of a long reach articulated carrier for inspection. In: Intelligent Robots and Systems, 2007. IROS 2007. IEEE/RSJ International Conference on, Oct. 29 2007-Nov. 2 2007 2007, pp. 4013-4019
10. Howard Allen, P.B.: Cylindrical Shell in Axial Compression. In: Background to Buckling. pp. 515 -524. McGraw-Hill Book Company (UK) Limited, (1980)
11. Hunter, D.F.: ESDU 88034 Avoidance of buckling of some engineering elements (struts, plates and gussets). In. IHS ESDU, (1988)